

## INFLUENCE OF LIGHT IRRADIATION ON ELECTRICAL AND OPTICAL PROPERTIES OF NANOCRYSTALLINE CADMIUM SELENIDE THIN FILMS

JEEWAN SHARMA<sup>\*</sup>, S K TRIPATHI<sup>a</sup>

*Department of Physics, Maharishi Markandeshwar University, Mullana, Ambala-133207 (India)*

*<sup>a</sup>Centre of Advanced Study in Physics, Panjab University, Chandigarh-160014 (India)*

The effect of light irradiation, on structural electrical and optical properties of nanocrystalline CdSe (n-CdSe) thin films synthesized by inert gas condensation technique (chamber pressure  $2 \times 10^{-1}$  mbar and temperature 298 K) has been investigated. The investigations are done using X-ray diffraction (XRD), optical transmission and conductivity measurements. The XRD study reveals the sphalerite cubic structure of the CdSe films with (111) as preferred direction. Transition from cubic to hexagonal phase has been observed after light irradiation. The structural parameters such as particle size, strain and dislocation density have been calculated. The absorption coefficient ( $\alpha$ ) and band gap ( $E_g$ ) are calculated using the transmission curves. Optical measurements indicate the existence of direct allowed optical transition with a decrease in energy gap after irradiation. The dark conductivity ( $\sigma_d$ ) and photoconductivity ( $\sigma_{ph}$ ) measurements indicate that the conduction in these materials is through an activated process having single activation energies.  $\sigma_d$  and  $\sigma_{ph}$  values increase with the increase in the crystallite size after irradiation. The values of carrier life time have been calculated and are found to increase with the increase in the particle size. Steady state photoconductivity ( $\sigma_{ph}$ ) measurements are done as a function of temperature and intensity.

(Received March 15, 2011; Accepted August 16, 2011)

*Keywords:* Inert gas condensation, Activation energy, photoconductivity and absorption coefficient.

### 1. Introduction

The synthesis of binary metal chalcogenides of group II–VI semiconductors in a nanocrystalline form is a rapidly growing area of research due to their important nonlinear optical properties, luminescent properties, quantum-size effect and other important physical and chemical properties [1]. In this group, cadmium selenide is a widely used semiconductor whose band gap lies in the solar energy spectrum. CdSe has been studied intensively in recent years because of its potential use as a photoanode in photoelectrochemical (PEC) cells [2]. By appropriate choice of CdSe nanocrystallite size the absorption edge can thus be made to fall anywhere in the visible region. Because of their interesting physical properties and device applications, many methods have been used to make CdSe nanocrystals.

On the other hand, decreasing size also implies an increase in the surface-to-volume ratio in the quantum dot, hence surface defects and dangling bonds are expected to play an increasing role.

Nanocrystalline thin films are attracting much attention because their properties, such as structural, optical and electrical, are changed by irradiation of photons, electron or ion beams. The

---

<sup>\*</sup>Corresponding author: jeewansharma29@gmail.com

photo induced changes on these thin films have potential use in large area thin film devices, such as light emitting devices, n-type window layer for thin film heterojunction solar cells and rear-window layer of thin film Si-based solar cells [3,4]. The physical properties of nanostructures are substantially influenced by the synthesis route and have a strong bearing on the microstructure of the specimens. Thermal evaporation of materials in the presence of a carrier gas is a technique, which is simple and less expensive. This technique has been utilized for the deposition of the metals and nanoclusters earlier [5]. The properties of nanomaterials are critically dependent on subsequent heat treatments like annealing in air, vacuum or different gaseous environments like H<sub>2</sub>, Ar, N<sub>2</sub> etc. [6]. The present paper reports the photo induced changes on the structural, electrical and optical properties of n-CdSe thin films prepared by inert gas condensation method.

## 2. Experimental details

The Semiconducting Cd<sub>30</sub>Se<sub>70</sub> was prepared from its constituents (5N pure) by melt-quenching technique as described earlier [7]. Thin films of this material were prepared in a conventional vacuum coating system on well degassed Corning 7059 glass substrates. These films were deposited in the presence of Ar gas at partial pressure of  $2 \times 10^{-1}$  mbar and temperature 298 K. Before the deposition, the vacuum chamber was evacuated to a vacuum of  $5 \times 10^{-6}$  mbar. The Ar gas was introduced into the chamber through specially designed inlet tube having a jet of diameter  $\sim 0.5$  mm. This jet was kept adjacent to the evaporation boat pointing towards the glass substrates. The vacuum chamber was purged several times with spectroscopic grade Ar gas to remove any residual gas impurities. Thermal evaporation of the material was carried out from the Mo boat. Crystallographic study was carried out using a Phillips PW-1610 X-ray diffractometer using CuK <sub>$\alpha$</sub>  radiation [ $\lambda=1.54056$  Å]. A monochromator-spectrograph (*SOLAR TII*, MS 2004) was used to study the optical transmission in CdSe thin films. The electrical measurements of these thin films were carried out in a specially designed metallic sample holder where heat filtered white light of intensity 8450 Lux (200 W tungsten lamp) was shown through a transparent glass window. A vacuum of about  $10^{-3}$  mbar was maintained throughout these measurements. Light intensity was measured using a digital luxmeter (*MASTECH*, MS6610). To monitor the changes due to light irradiation, the prepared thin film was irradiated with the heat filtered white light having intensity 8450 Lux for four hours. After relaxation of the sample for 24 hours, the electrical and optical measurements were performed.

### 2.1 Structural

Information of the strain and the particle size are obtained from the full widths at half maximum (FWHM) of the diffraction peaks. The FWHM ( $\beta$ ) can be expressed as a linear combination of the contributions from the strain ( $\epsilon$ ) and particle size ( $L$ ) through the following relation [8]

$$\frac{\beta \cos \theta}{\lambda} = \frac{1}{L} + \frac{\epsilon \sin \theta}{\lambda} \quad (1)$$

The lattice spacing  $d$  is calculated using the Bragg's formula

$$2d \sin \theta = n\lambda \quad (2)$$

The lattice parameter 'a' is determined for cubic structure by using the expression:

$$d^2 = \frac{a^2}{(h^2 + k^2 + l^2)} \quad (3)$$

where  $h$ ,  $k$  and  $l$  represent the lattice planes.

## 2.2 Optical

The fundamental absorption, which corresponds to the transition from valence band to conduction band, can be used to determine the band gap of the material. The relation between  $\alpha$  and the incident photon energy ( $h\nu$ ) can be written as [9]

$$\alpha = \frac{A(h\nu - E_g)^n}{h\nu} \quad (4)$$

where  $A$  is a constant,  $E_g$  is the band gap of the material and the exponent  $n$  depends on the type of transition. The  $n$  may have values 1/2, 2, 3/2 and 3 corresponding to the allowed direct, allowed indirect, forbidden direct and forbidden indirect transitions, respectively.

## 2.3 Electrical

Planar geometry of the films (length  $\sim 1.0$  cm; electrode gap  $\sim 8 \times 10^{-2}$  cm) was used for the electrical measurements. Pre deposited thick Indium electrodes were used for the electrical contacts. The electrical conductivity in thin film has been calculated using two probe method. The activation energy is calculated by typical Arrhenius equation:

$$\sigma_d = \sigma_o \exp\left(\frac{-\Delta E}{kT}\right) \quad (5)$$

where  $\Delta E$  is the activation energy for conduction and  $k$  is the Boltzmann's constant. The photocurrent ( $I_{ph}$ ) was obtained after subtracting the dark current ( $I_d$ ) from the current measured in the presence of light. For transient photoconductivity measurements, light was shone on the thin film and, the rise and decay of photocurrent was noted manually from a digital picoammeter (DPM-11 Model). The accuracy in  $I_{ph}$  measurements was typically 1 pA.

## 3. Results and discussion

### 3.1 Structural analysis

The XRD pattern of the as-deposited and irradiated n-CdSe thin films on glass substrates has

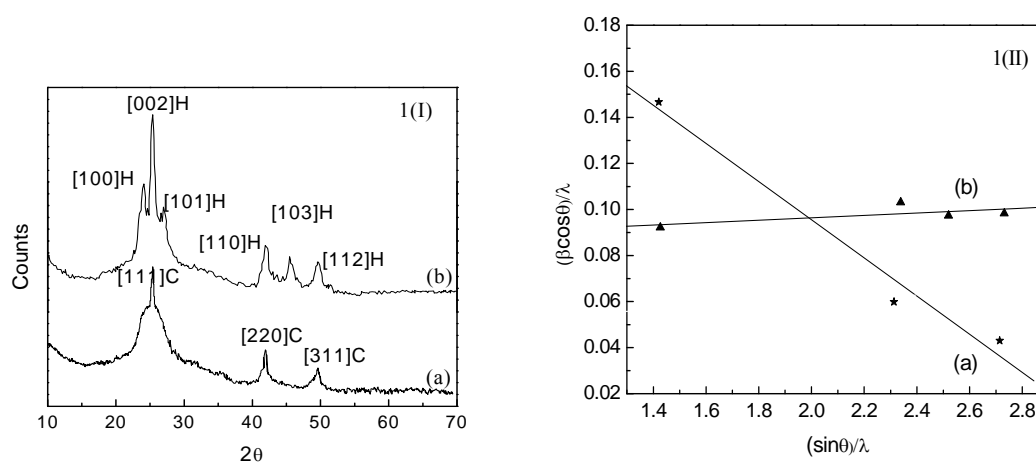


Fig. 1: (I) The XRD pattern and (II) Plot between  $(\beta \cos \theta) / \lambda$  and  $(\sin \theta) / \lambda$  for (a) as-deposited and (b) irradiated CdSe thin films.

been shown in figure 1(I). The spectrum of as-deposited film have highest intensity diffraction peak at  $2\theta = 25.3^\circ$  (111) with two other small intensity peaks at  $2\theta = 41.8^\circ$  (220) and  $49.5^\circ$  (311) indicating that (111) is preferred orientation. The (111) direction is the close packed direction of zinc-blende and the as-deposited films are polycrystalline having sphalerite cubic structure. Some new peaks at  $2\theta = 24.1^\circ$  (100),  $27.4^\circ$  (101) and  $45.9^\circ$  (103) are observed after light irradiation. The intensity of main peak is increased after irradiation, indicating increase in crystalline size. The comparison of observed 'd' values with standard 'd' values [10,11] confirms that the as-deposited films have zinc-blende type structure and the new peaks arise due to presence of more stable hexagonal phase in irradiated films.

Table 1: Structural parameters for as-deposited and irradiated n-CdSe thin films.

Pressure (mbar)	$2\theta$ (deg.)	h k l	Lattice spacing 'd' (Å)	Lattice parameter 'a' (Å)	Particle size 'L' (nm)	Strain ' $\epsilon$ ' ( $\text{lin}^{-2} \text{m}^{-4}$ )
As-deposited	25.29	111	3.528	6.111	03.92	$-8.13 \times 10^{-2}$
	41.81	220	2.164			
	49.51	311	1.844			
Irradiated	23.96	100	3.711		12.12	$5.23 \times 10^{-3}$
	25.40	002	3.505			
	27.14	101	3.284			
	42.22	110	2.139			
	45.69	103	1.984			
	49.77	112	1.831			

The plot between  $(\beta \cos \theta) / \lambda$  and  $(\sin \theta) / \lambda$ , for both n-CdSe films, have been shown in figure 1(II). The structural parameters of n-CdSe thin films before and after irradiation are listed in table 1. The change in lattice parameter for films over bulk clearly indicates that the grains are strained. This may be due to the change of nature and concentration of native imperfections [12]. The negative value of residual strain for the as-deposited film indicates the compressive strain. The irradiated film has positive values of residual strain indicating the strain in this film is tensile. If the deposited film is free from impurities, the compressive strain is generated at the thin film substrate interface, when the very small crystallites are bonded to substrates due to surface tension effect. The tensile strain developed in irradiated film may be due to the difference in thermal expansion coefficients of the substrate and deposited material. The decrease in strain after light irradiation may be attributed to the improvement in the crystallinity of the film and presence of more stable hexagonal phase in the.

### 3.2 Optical analysis

The variation of percentage transmission with wavelength for both n-CdSe thin films has been shown in figure 2(I). There is a sharp fall of transmittance curve at the band edge which confirms the crystalline nature deposited films. From the transmission data, nearly at the fundamental absorption edge, the absorption coefficient ( $\alpha$ ), are calculated in the region of strong absorption using the relation

$$\alpha = \frac{1}{d} \ln \left( \frac{1}{T} \right) \quad (6)$$

To check the transition type in films the values of n have been calculated by the procedure described elsewhere [13]. The value of n is calculated to be 0.49 and 0.60 for as-deposited and irradiated thin films, indicating that the transition is direct. Figure 2(II) shows the plots between  $(\alpha h\nu)^2$  and  $h\nu$  for both cases. The energy band gap is found to be  $(2.22 \pm 0.01)$  eV and  $(2.03 \pm 0.01)$  eV for as-deposited and irradiated thin films. The band gap decreases after irradiating the film which is likely due to increase in crystalline size and decrease in quantum confinement.

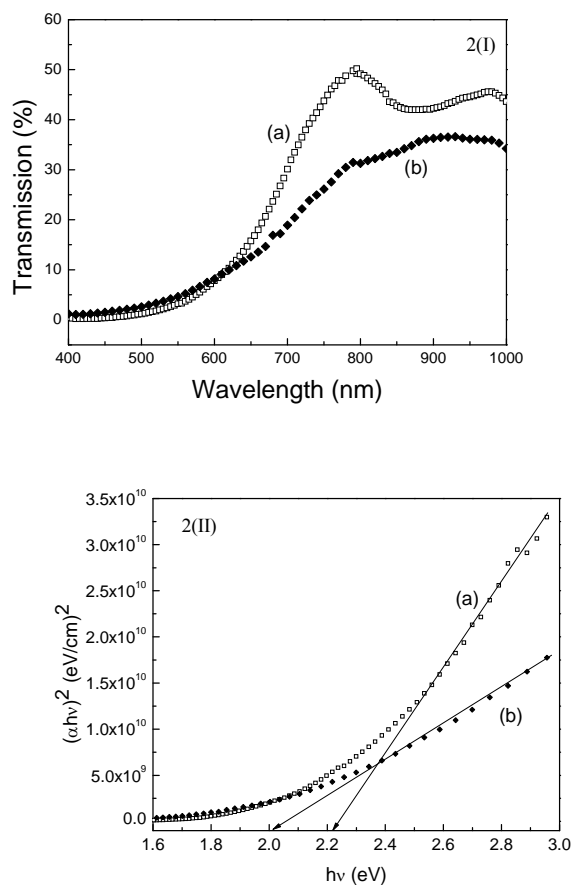


Fig. 2. (I) Transmission data and (II) Variation of  $(\alpha h\nu)^2$  with energy for (a) as-deposited and (b) irradiated n-CdSe thin films.

### 3.3 Electrical analysis

The temperature dependence of dark conductivity for n-CdSe thin films have been shown in figure 3(I). The plots between  $\ln \sigma_d$  and  $1000/T$  are straight lines in both cases indicating that conduction is an activated process having single activation energy ( $\Delta E_d$ ) in the observed temperature range (253-358 K). The value of  $\Delta E_d$  is obtained from the slopes of the plots {figure 3(I)}. The values of  $\sigma_d$  and  $\Delta E_d$  increase after light irradiation.

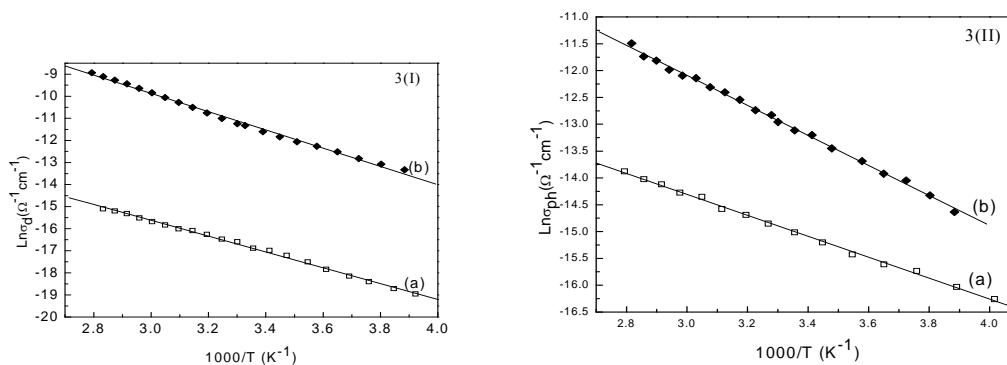


Fig. 3. Temperature dependence of (I) dark conductivity and (II) photo conductivity for (a) as-deposited and (b) irradiated n-CdSe thin films.

The values of  $\sigma_d$  and  $\Delta E_d$  are listed in table 2. The increase in conductivity can be attributed to decrease in surface scattering including grain boundary scattering due to increase in crystallite size. Figure 3(II) shows the temperature dependence of photo conductivity for n-CdSe thin films. The photoconductivity is an activated process and the activation energy for photoconduction ( $\Delta E_{ph}$ ) is much smaller than for dark conduction. The value of photo activation energy is calculated from the slopes of the curves {figure 3(II)}. The values of  $\sigma_{ph}$  and  $\Delta E_{ph}$  increase after light irradiation (Table 2).

Table 2: Representation of dark-, photo-conductivity, dark-, photo-activation energy and carrier life time for as-deposited and irradiated n-CdSe thin films.

Film ( $\ln\tau_d$ ) <sub>t=0</sub>	$\sigma_d$ ( $\Omega^{-1} \text{ cm}^{-1}$ )	$\sigma_{ph}$ ( $\Omega^{-1} \text{ cm}^{-1}$ )	$\Delta E$ (eV)	$\Delta E_{ph}$ (eV)	
As-deposited.	$(4.62 \pm 0.02) \times 10^{-8}$	$(2.93 \pm 0.02) \times 10^{-7}$	$(0.31 \pm 0.01)$	$(0.17 \pm 0.01)$	1.3
Irradiated	$(9.96 \pm 0.02) \times 10^{-6}$	$(2.36 \pm 0.02) \times 10^{-6}$	$(0.37 \pm 0.01)$	$(0.24 \pm 0.01)$	1.8

The rise and decay of photocurrent at room temperature (298 K) for both cases is shown in figure 4(I). The photocurrent first rises and then settles down to a steady state value. It is also observed that the decay of photocurrent is quite slow and a persistent photocurrent is observed. It is believed that the persistent photocurrent may not be simply due to carriers trapped in the localized states [14]. In order to simplify the analysis, the persistent photocurrent is subtracted from the measured photocurrent. Decay becomes slower when n-CdSe film is irradiated with light.

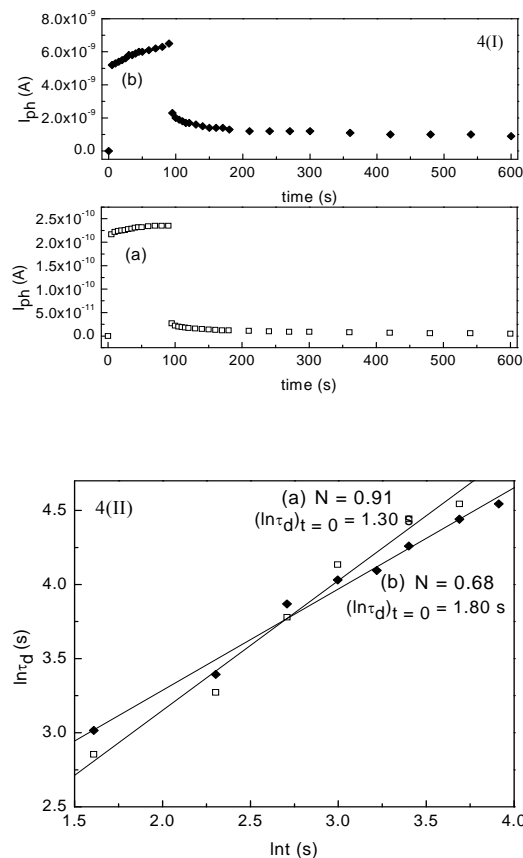


Fig. 4. (I) Rise and decay of photocurrent and (II)  $\ln\tau_d$  as a function of  $\ln t$  for (a) as-deposited and (b) irradiated CdSe thin films.

To study the decay rate analysis quantitatively, the decay time constant ( $\tau_d$ ) have been calculated using relation [15,16]

$$\tau_d = - \left[ \frac{1}{I_{ph}} \left( \frac{dI_{ph}}{dt} \right) \right]^{-1} \quad (7)$$

where  $I_{ph}$  is the maximum photocurrent at  $t = 0$  for a given applied voltage. The value of  $\tau_d$  increases with time in all the cases at room temperature and intensity 8450 Lux, which confirms the non-exponential decay of photocurrent. For exponential decay, the decay constant should not vary with time. The plots between  $\ln \tau_d$  and  $\ln t$  are straight lines {figure 4(II)}, which obey a power law of the form  $t^N$ , with  $N = d(\ln \tau_d / \ln t)$  and the value of  $N$  is calculated to be 0.91 and 0.84 for as-deposited and irradiated films respectively. The extrapolation of these straight lines at  $t = 0$ , gives the value of carrier life time for as-deposited and irradiated films (Table 2). The observed slow decay process is due to the presence of the deep localised states in this material. The decay in photocurrent becomes slower for light irradiated film. Since optical energy gap ( $E_{opt}$ ) of n-CdSe is 2.22 eV, so the absorbed photon energy (theoretically excess energy) can be converted to heat energy (phonon) by the lattice scattering in thin film. Therefore, it can be thought that the primary factor in this photo induced transition is the thermal effect.

The density of thin film is known to decrease due to the presence of a large number of defects, which are simulated as voids using the EMA [19]. Simultaneously, the reduction in particle size leads to an increased level of disorder in the system. This is understandable since reduction in the grain size results in a larger fraction of atoms residing at the grain boundaries than with in the grain. With the presence of voids, the extent of defects like dangling bonds present in the surface should lead to a slow decay of photocurrent.

#### 4. Conclusions

Nanocrystalline CdSe thin films are deposited on well degassed corning glass substrates using inert gas condensation technique. Nanocrystalline nature of films has been confirmed using X-ray diffraction. The structure of deposited films was cubic with (111) as preferred orientation. Transition from cubic to more stable hexagonal phase and increase in crystalline quality has been observed after light irradiation. Strain in the film is found to decrease after light irradiation. The transition in both the films was found to be direct. The optical band gap value decreases after light irradiation. Steady state photoconductivity studies indicate that there is a continuous distribution of localised states. Decay of photocurrent is slow due to deeper localised states present in this material. Decay of photocurrent becomes slower after irradiation due to the increase in the number of localized states.

#### Acknowledgements

The experimental work has been performed in Department of Physics, Panjab University Chandigarh. We acknowledge the financial support provided by the CSIR, New Delhi for the completion of this work.

#### References

- [1] C. Gan, Y. Zhang, S.W. Liu, Y. Wang, M. Xiao, *Optical Materials*, **30**, 1440 (2008).
- [2] Y.G. Gudage, Ramphal Sharma, *Current Applied Physics*, **10**, 1062 (2010).
- [3] K. Winz, C.M. Fortmann, T. Eickhoff, C.B. King, H. Wagner, H. Fujiwara, I. Shimizu, *Solar Energy Mater. Solar Cells*, **49**, 195 (1997).
- [4] J.M. Dona, J. Herrero, *J. Electrochem. Soc.*, **142**, 764 (1995).
- [5] M. Tanaka, A. Sawai, M.M. Sengoku, M. Kato, Y. Masumoto, *J. Appl. Phys.*, **87**, 8535 (2000).
- [6] R.B. Kale, C.D. Lokhande, *Appl. Surf. Sci.*, **223**, 343 (2004).

- [7] J. Sharma, G.S.S. Saini, N. Goyal, S.K. Tripathi, *Journal of Optoelectronics and Advanced Materials*, **9**, 3194 (2007).
- [8] S.B. Qadri, E.F. Skelton, D. Hsu, A.D. Dinsmore, J. Yang, H.F. Gray, A.D. Ratna, *Phys. Rev. B*, **60**, 9191 (1999).
- [9] J.I. Pankove, *Optical Processes in Semiconductors*, Englewood Cliffs., NJ: Prentice-Hall (1971).
- [10] JCPDS Data file no. 8-459.
- [11] JCPDS Data file no. 19-191.
- [12] K. Reichelt, X. Jiang, *Thin Solid Films*, **191**, 91 (1990).
- [13] J. Sharma, G. Singh, A. Thakur, G.S.S. Saini, N. Goyal, S.K. Tripathi, *Journal of Optoelectronics and Advanced Materials*, **7**, 2085 (2005).
- [14] V. Sharma, A. Thakur, P.S. Chandel, N. Goyal, G.S.S. Saini, S.K. Tripathi, *J. Optoelectron. Adv. Mater.*, **5**, 1243 (2003).
- [15] W. Fuhs, D. Meyer, *Phys. Stat. Solidi (a)*, **24**, 275 (1974).
- [16] A. Kumar, S. Goel, S.K. Tripathi, *Phys. Rev. B*, **38**, 13432 (1988).
- [17] G.W. Mbise, D.L. Bellac, G.A. Niklasson, C.G. Granqvist, *J. Phys. D: Appl. Phys.* **30**, 2103 (1997).